# Decoupled, Reduced Order Model For Double Output Induction Generator Using Integral Manifolds and Iterative Seperation Theory

M. Kalantar
Associate professor

M. Sedoghizadeh
Ph.D. Student

Electrical Faculty-Iran University of Science and Technology-Narmak

## Abstract

*A technique is presented and confirmed for developing the computational efficiency in simulating double output induction generators with two rotor circuits where stator transients are to be included. Iterative decomposition is used to separate the flux–Linkage equations into decoupled fast and slow subsystems, after which the model order of the fast subsystems is reduced by neglecting the heavily damped fast transients caused by the second rotor circuit using integral manifolds theory. The two decoupled subsystems along with the equation for the very slowly changing slip constitute a three time-scale model for the machine which resulted in increasing computational speed. Finally, the proposed method of reduced order in this paper is compared with the other conventional methods in both linear and nonlinear equations and it is shown that this method is better than the other methods regarding simulation accuracy and speed.*

## Key words

*DOIG, Integral Manifolds, Reduced order, Iterative Seperation*

## Introduction

Wind energy conversion systems have in the past two decades been the object of strong interest as a viable source of electrical energy. Various electromechanical schemes for generating electricity from the wind have been suggested. Variable speed generation schemes offer a number of advantages when compared with fixed speed induction generation. At a given wind speed, higher energy capture is possible by maximizing turbine effciency through adjustment of shaft speed. Reduction of the torque ripple in the drive train and torsional mode resonance can also be achieved with adjustable speed operation. One such variable speed scheme is the static Kramer drive, also referred to as the subsynchronous converter cascade, which when mechanically driven above synchronous speed will operate as a generator i.e. double output induction generator(DOIG). The system in its conventional form is showen in Fig. 1. It consist of a wound rotor induction machine connected through its slip rings to a three phase diode bridge rectifier and a line commutated inverter connected to the ac supply via a step up transformer[1-3].

Electromechanical transients of double output induction generators(DOIG) are usually simulated digitally using state variables and a point by point time domain solution. The underlying assumptions and the degree of detail of the machine model used for the simulation are dependent on the particular type of application . For instance , in transient stability studies of power systems , high-frequency oscillatory transients of the active and reactive powers caused by the machine stator winding are usually ignored.

However , there are several applications such as power system studies of short circuits , relay coordination , sub synchronous resonance , switching transients and shaft stresses , where machine stator (and network) transients should be included[4] .

Such studies require considerable computational effort since the cpu time is related not only to the square of the model order, but also to the integration time step which has to be relatively small due to the fast oscillatory transients.

In this paper, a procedure is presented to reduce computational effort when stator transients of DOIG's are be included. The method is developed by judicious interpretation of the physical phenomena involved, decomposition of the transients into fast and slow parts, and model order reduction by neglecting heavily damped fast transients using integral manifolds.

Large DOIG's are generally equipped with a two rotor circuits (double cage) or deep-bar rotor. In the following, a double-cage DOIG will be considered.

The resulting model, however, can also be applied with some degree of approximation to DOIG's with deep-bar rotors since an equivalent double cage can always be found which provides the machine with an admittance locus closely fitting that of a deep-bar induction machine [5] .

In a first step, some of the methodologies currently available to reduce the order of power systems models have been applied to the induction machine.

With the aim of gainig some insight regarding the behavior of each technique, a steady state preliminary analysis has been carried out, using linearized models in order to take advantage of its inherent simplicity[6].

Modal truncation is one first reduction schemes that has been applied to electric power systems[7]. This technique is based on the pole location of the system. The state variables are transformed in modal variables and the fast decay poles and/or those associated with high frequencies are neglected, thus enabling a reduction in the order of the system .

Balanced reduction techniques take a slightly different approach, because they are based in the input/output behavior of the system [8]. Actually, the original state-space system is transformed into a new representation that has the property that each state-space variable is both controllable and observable. In order to achieve a reduced order model, states that are strongly influenced by the inputs and storngly connected to the outputs are retained , whereas states that are weakly controllable and observable are truncated.

Another method used in power systems order reduction is the so called optimal Hankel-norm approximation [9]. This criterion tries achieve a compromise between a small worst case error and a small energy error.

Another technique used in power system as singular perturbations decomposes the system according to its fast and slow dynamics and then lowers the model order by first neglecting the fast dynamics phenomena [10]. The effect of fast dynamics are then reintroduced as boundary layer correction calculated in separated time scales, which leads to correct static gains.

The technique known in the literature is the concept of iterative seperation[11] and integral manifolds, a nonlinear generalization of the notion of invariant subspace in linear systems[12]. This paper employs the manifold concept as a tool for reduced order modeling and decomposition of DOIG.

## 1- Doig Full Order Model

In this paragraph, the equations describing the subsystems of a variable speed wind turbine with DOIG and converter (rectifier+inverter) will be developed. The equations for the rotor, the generator and the converter will be given here. The equations have been developed using the following assumptions:

-All rotating mass is represented by one element. The so-called 'lumped-mass' representation. Elastic shafts and resulting torsional forces are neglected.

-Magnetic saturation in the DOIG is neglected.

-Dynamic phenomena in the converter are neglected

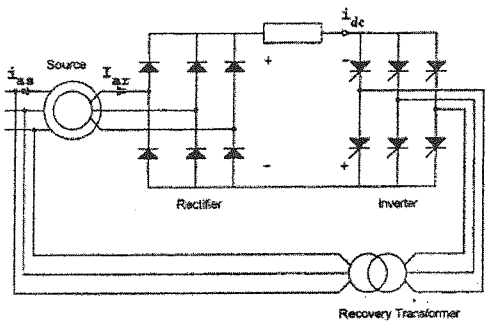


**Figure (1) shematic representation of DOIG.**

Using the subscripts 1,2 and 3 to refer to the stator winding, first and second circuits respectively, the d,q equations in per-unit for the flux linkages of a DOIG with two rotor circuit can be expressed in the synchronously revolving reference frame [13] as follows (see appendix for notations and parameters not defined in the text):

$$\begin{aligned}\varphi_{1d}^{\bullet} &= -(r_1 l_{11}/l)\ \varphi_{1d} + \omega\varphi_{1q} + (r_1 l_3 l_m/l)\varphi_{2d} + (r_1 l_2 l_m/l)\varphi_{3d} + v_{1d}\\ \varphi_{1q}^{\bullet} &= -\omega\varphi_{1d} - (r_1 l_{11}/l)\ \varphi_{1q} + (r_1 l_3 l_m/l)\varphi_{2q} + (r_1 l_2 l_m/l)\varphi_{3q} + v_{1q}\end{aligned} \tag{1}$$

$$\begin{aligned}\varphi_{2d}^{\bullet} &= [(r_2 + R_c)(l_3 l_m/l) + R_c l_2 l_{33}/l]\varphi_{1d} - [(r_2 + R_c)(l_{22}/l) - l_1 l_m R_c/l]\varphi_{2d}\\ &+ s\omega\varphi_{2q} + [(r_2 + R_c)(l_1 l_m/l) + R_c l_{33}/l]\varphi_{3d} + v_{2d}\\ \varphi_{2q}^{\bullet} &= [(r_2 + R_c)(l_3 l_m/l) + R_c l_2 l_{33}/l]\varphi_{1q} - s\omega\varphi_{2d}\\ &- [(r_2 + R_c)(l_{22}/l) - l_1 l_m R_c/l]\varphi_{2q} + [(r_2 + R_c)(l_1 l_m/l) + R_c l_{33}/l]\varphi_{3q} + v_{2q}\end{aligned} \tag{2}$$

$$\begin{aligned}\tau_3\varphi_{3d}^{\bullet} &= [(1+R_c/r_3)(l_2 l_m) + R_c l_3 l_m/r_3]\varphi_{1d} + [(1+R_c/r_3)(l_1 l_m)\\ &- R_c l_{22}/r_3]\varphi_{2d} - [(1+R_c/r_3)(l_{33}) + R_c l_3 l_m/r_3]\varphi_{3d} + (s\omega l/r_3)\varphi_{3q}\\ \tau_3\varphi_{3q}^{\bullet} &= [(1+R_c/r_3)(l_2 l_m) + R_c l_3 l_m/r_3]\varphi_{1q} + [(1+R_c/r_3)(l_1 l_m)\\ &- R_c l_{22}/r_3]\varphi_{2q} - (s\omega l/r_3)\varphi_{3d} - [(1+R_c/r_3)(l_{33}) + R_c l_3 l_m/r_3]\varphi_{3q}\end{aligned} \tag{3}$$

$$T_e = (l_3 l_m/l)(\varphi_{1d}\varphi_{2q} - \varphi_{1q}\varphi_{2d}) + (l_2 l_m/l)(\varphi_{1d}\varphi_{3q} - \varphi_{1q}\varphi_{3d}) \tag{4}$$

where

$$\tau_3 = l/r_3 \tag{5}$$

due to existance of the common end-ring in the double cage DOIG used in this study, equations (1)-(3) contain terms which describe voltage drop on common resistance $R_c$.

$$s^{\bullet} = (\omega/2H)(T_e - T_l) \tag{6}$$

$$T_l = K\omega_r^2 \tag{7}$$

where $K$ corresponds to full load.

The slip equation is highly nonlinear. Linearization of this equation for the purpose of mode decoupling would time consuming because the operating point of the flux linkages would have to be continually re-evaluated during the simulation. However, due to the ralatively large mechanical time constant, the nonlinear slip equation step even though fast changing flux-linkages obtained from the flux –linkage equations are used.

The flux-linkage equations may be linearized at some slip value and therefore can be treated as linear provide the slip is updated in a timely manner. Each of the flux linkages $\varphi_1$, $\varphi_2$, and $\varphi_3$ contains a predominant mode almost equal to its own natural mode. Fast parts in transients generally arise from high-frequency, lightly damped modes such as the predominant mode in $\varphi_1$, or form modes that are heavily damped, such as the predominant mode in $\varphi_2$. The slow part of the flux-linkage transients in the case considered , assuming sufficiently low slip, is the predominant mode in $\varphi_3$. Sufficiently low absolute slip values will be implicitly assumed in the model development.

Thus $\varphi_1$ and $\varphi_2$ contain mainly fast transients whereas $\varphi_3$ is predominantly slow. Since the fast transient parts of $\varphi_3$ are small compared with its slow part as well as with the fast transient parts of $\varphi_1$ and $\varphi_2$, equations (1), (2) and (3) are state separable, i.e.the fast and slow modes can be separated by and iterative process. This will convert the sixth order flux-linkage equations into a set of simultaneous fourth order equations for the fast trasnsients and a set of simultaneous second order equations for the slow transients. These seperated stes of equations, along with the equation for the very slowly changing slip, provide a simulation model which will reduce the computational effort if the integration time steps for the three subsystems are properly selected.

## 2-Iterative Separation of Slow and Fast Modes

Grouping the machine flux-linkages into the predominantly fast changing flux linkages of the stator winding and second rotor circuit

$$\varphi_{ss} = [\varphi_{1d} \cdots \varphi_{1q} \cdots \varphi_{3d} \cdots \varphi_{3q}] \tag{8}$$

and the predominantly slowly varying flux-linkages of the first rotor circuit

$$\varphi_r = [\varphi_{2d} \cdots \varphi_{2q}] \tag{9}$$

equations (1), (2) and (3) can be written in partitional from as

$$\begin{bmatrix} \varphi^{\bullet}_{ss} \\ \varphi^{\bullet}_{r} \end{bmatrix} = \begin{bmatrix} A \cdots\cdots\cdots B \\ C \cdots\cdots\cdots D \end{bmatrix} \begin{bmatrix} \varphi_{ss} \\ \varphi_r \end{bmatrix} + \begin{bmatrix} v_1 \\ v_2 \end{bmatrix} \tag{10}$$

$$v_1 = \begin{bmatrix} v_{1d} \\ v_{1q} \\ \\ 0 \\ 0 \end{bmatrix} \cdots\cdots v_2 = \begin{bmatrix} v_{2d} \\ v_{2q} \end{bmatrix}.$$

To better isolate the fast and slow modes from each other, it is necessary to reduce the effect of the slowly varying part of $\varphi_r$ on $\varphi_{ss}$, and the effect of the fast varying part of $\varphi_{ss}$ on $\varphi_r$. This is equivalent to reducing the coupling matrices $B$ and $C$ in equation (10), which will be carried out iteratively.

First, defining $\varphi^{o}_{ss}$. As the quasi-steady state valued for $\varphi_{ss}$ by setting $\varphi^{\bullet}_{ss}$ to zero in equation (10) gives

$$\varphi^{0}_{ss} = -A^{-1}B\varphi_r - A^{-1}v_1 \tag{11}$$

Thus, $\varphi_{ss}^{o}$ is the value of $\varphi_{ss}$ if $\varphi_{ss}$ were instantly damped. To remove the slowly varying part of $\varphi_{ss}$, is introduced as the difference between $\varphi_{ss}$ and $\varphi_{ss}^{o}$ from (11):

$$\mu_1 = \varphi_{ss} + A^{-1}B\varphi_r + A^{-1}v_1 \tag{12}$$

Substituting $\varphi_{ss}$ from (12) in (10) and ignoring the $s^{\bullet}$ terms in $A^{\bullet}$ ( since, as noted earlier, s is very slowly varying ), yield

$$\mu_1^{\bullet} - A^{-1}v_1^{\bullet} = A_1\mu_1 + B_1\varphi_r - A^{-1}BCA^{-1}v_1 \tag{13}$$

and

$$\varphi_r^{\bullet} = C\mu_1 + D_1\varphi_r + v_2 - CA^{-1}v_1 \tag{14}$$

with

$$A_1 = A + A^{-1}BC \ldots\ldots B_1 = A^{-1}BD \ldots\ldots D_1 = D - CA^{-1}B \tag{15}.$$

Introducing

$$\eta_1 = \mu_1 - A^{-1}v \tag{16}$$

Or, considering (12),

$$\eta_1 = \varphi_{ss} + A^{-1}B\varphi_r \tag{17}$$

where $\eta_1$ is as fast as $\mu_1$, equations (13) and (14) become

$$\eta_1^{\bullet} = A_1\eta_1 + B_1\varphi_r + v_1 \tag{18}$$

and

$$\varphi_r^{\bullet} = C\eta_1 + D_1\varphi_r + v_2 \tag{19}.$$

Equations (18) and (19) are similar to (10) except that $\eta_1$ has replaced $\varphi_{ss}$ and the effect of $\varphi_r$ on the equation is attenuated since it can be shown that the elements of $B_1$ are smaller than those of $B$.
To Further reduce the effect of $\varphi_r$, the attenuation process is repeated by defining, as in (17),

$$\eta_2 = \eta_1 + A_1^{-1}B_1\varphi_r \tag{20}$$

And subsequent substitution of $\eta_1$ from (20) into (18) and (19):

$$\eta_2^{\bullet} = A_1\eta_2 + B_2\varphi_r + v_1 \tag{21}$$

$$\varphi_r^{\bullet} = C\eta_2 + D_2\varphi_r + v_2 \tag{22}$$

Where

$$A_2 = A_1 + A_1^{-1}B_1C.....B_2 = A_1^{-1}B_1D_2...D_2 = D_1 - CA_1^{-1}B_1 \tag{23}$$

Equations (21) and (22) have replaced (18) and (19) but now the effect of $\varphi_r$ is more attenuated because $B_2$ is smaller than $B_1$.

In general, if the attenuation process is carried out $n$ times, the resulting equations are

$$\eta_n^{\bullet} = A_n\eta_n + B_n\varphi_r + v_1 \tag{24}$$

and

$$\varphi_r^{\bullet} = C\eta_n + D_n\varphi_r + v_2 \tag{25}$$

Where

$$\eta_n = \eta_{n-1} + A_{n-1}^{-1}B_{n-1}\varphi_r \tag{26}$$

With

$$A_n = A_{n-1} + A_{n-1}^{-1}B_{n-11}C..... B_n = A_{n-1}^{-1}B_{n-1}D_n....D_n = D_{n-1} - CA_{n-1}^{-1}B_{n-1} \tag{27}$$

The coupling of the fast variable $\eta_n$ into the slow variable $\varphi_r$ equation in (25) is still $C$. To reduce this coupling by iterative separation, $\eta_n$ is eliminated in equations (24) and (25):

$$\varphi_r^{\bullet} - CA_n^{-1}\eta_n^{\bullet} = (D_n - CA_n^{-1}B_n)\varphi_r - CA_n^{-1}v_1 + v_2 \tag{28}$$

The right hand side of (28) contains less of the fast transients than the right hand side of (25) since is $\eta_n$ eliminated. Thus, the vaiable

$$\sigma_1 = \varphi_r - CA_n^{-1}\eta_n \tag{29}$$

Contains less fast transients than $\varphi_r$, substituting $\varphi_r$ from (29) into (24) and (25), and ignoring the $s^{\bullet}$ terms in $A^{\bullet}$ yield

$$\eta_n^{\bullet} = A_{n1}\eta_n + B_{n1}\sigma_1 + v_1 \tag{30}$$

And

$$\sigma_1^{\bullet} = C\eta_n + D_{n1}\sigma_1 - F_{n1}v_1 + v_2 \tag{31}$$

With

$$A_{n1} = A_n + B_nCA_n^{-1}....C_1 = D_{n1}CA_{n1}^{-1}....$$
$$D_{n1} = D_n - CA_n^{-1}B_n....F_{n1} = CA_n^{-1}$$

Carrying out the iterative decoupling process of the fast transients from the slow variable

equation $m$ times results in

$$\eta_n^{\bullet} = A_{nm}\eta_n + B_n\sigma_m + v_1 \tag{32}$$

and

$$\sigma_m^{\bullet} = C_m\eta_n + D_{nm}\sigma_m - F_{nm}v_1 + v_2 \tag{33}$$

Where

$$\sigma_m = \sigma_{m-1} - C_{m-1}A_{nm-1}^{-1}\eta_n \tag{34}$$

With

$$\begin{aligned} &A_{nm} = A_{nm-1} + B_nC_{m-1}A_{nm-1}^{-1}....C_m = D_{nm}C_{m-1}A_{nm-1}^{-1}.... \\ &D_{nm} = D_{nm-1} - C_{m-1}A_{nm-1}^{-1}B_n....F_{nm} = C_{m-1}A_{nm-1}^{-1}....F_{n0} = 0 \end{aligned} \tag{35}$$

It can be shown that at sufficiently low absolute slip values, the elements of $B_n$ and $C_m$ approach zero as $n$ and $m$ go to infinity for typical machine parameters. Generally, the convergence of this iteration process is quite fast. if $B_n$ and $C_m$ are sufficiently small, equations (32) and (33) can be simulated in decoupled from as

$$\eta_n^{\bullet} = A_{nm}\eta_n + v_1 \tag{36}$$

And

$$\sigma_m^{\bullet} = D_{nm}\sigma_m - F_{nm}v_1 + v_2 \tag{37}$$

However, a small steady-state error is created by ignoring $B_n$ and $C_m$. This can be compensated by inserting the steady state variables $\eta_n^o$ and $\varepsilon_m^o$ in (36) and (37) as follows:

$$\eta_n^{\bullet} = A_{nm}\eta_n + B_n\sigma_m^0 + v_1 \tag{38}$$

$$\sigma_m^{\bullet} = C_m\eta_n^0 + D_{nm}\sigma_m - F_{nm}v_1 + v_2 \tag{39}$$

From which $\eta_n^o$ and $\eta_n^o$ can be found by setting $\eta_n^{\bullet} = \varepsilon_m^{\bullet} = 0$. The result can be written as

$$\eta_n^{\bullet} = A_{nm}\eta_n + G_{nm}v_1 \tag{40}$$

And

$$\sigma_m^{\bullet} = D_{nm}\sigma_m - H_{nm}v_1 + v_2 \tag{41}$$

Where

$$G_{nm} = B_nD_{nm}^{-1}H_{nm} + I.....H_{nm} = C_mA_{nm}^{-1}G_{nm} + F_{nm} \tag{42}$$

From which $G_{nm}$ and $H_{nm}$ can be solved.

## 3-Neglecting Heavily Damped Fast Transients Using Integral Manifolds

### 3-1-Integral Manifolds Theory

A smooth s-dimensional surface $S$ in the n-dimensional space $R^n$ is defined by $m=n-s$ independent algebraic or transcendental scalar equations. In their simplest form, these equations express certain $m$ coordinates $z$ as $m$ explicit functions of the remaining s coordinates $x$, that is they define S by its graph:

$$S: z=h(x)\ ,\ z\in R^m\ ;\ x\in R^s\ ;\ m+s=n \tag{43}$$

It is assumed that, for all $x$ in a domain of practical interest, $\partial h/\partial x$ exists and has full rank $m$. For approximated constructions of $h(x)$ pursued in this paper it will also be assumed that higher order derivatives of $h(x)$ exist and are continuous. In a more general situation the surface $S$ may vary with time $t$, then

$$S_t: z=h(x,t)\quad ,\ z\in R^m\ ;\ x\in R^s\ ;\ m+s=n \tag{44}$$

It will be assumed that $\partial h/\partial t$ exists and is continuous over an interval of interest $t\in(t_0,t_1)$, preferably infinite:

$$t_1\to\infty$$

Let us now use the same coordinates $z$ and $x$ to describe a dynamic system $D_t$ in $R^n$:

$$z^{\bullet}=g(x,z,t),\ldots\ldots\ldots z\in R^m \tag{45}$$

$$x^{\bullet}=f(x,z,t),\ldots\ldots\ldots z\in R^s, m+s=n \tag{46}$$

Where appropriate differentiability assumptions are made about $g$ and $f$. The surface $S_t$ ,and the system $D_t$ have thus been introduced as two entities unrelated to each other. In this paper we explore a particulary useful relationship of $s_t$ and $D_t$: when $S_t$ is an integral manifold of $D_t$. The term invariant manifold will be used when such an integral manifold is time-invariant, that is when $\partial h/\partial t = 0$ and $S_t=S$ as in (43).

***Manifold Definition***: Surface $S_t$ is an integral manifold of $D_t$ if every solution $z(t)$, $x(t)$, of (45) – (46) which is in $S_t$ at $t=t_0$.

$$Z(t_0)=h(x(t_0)\ ,\ t_0) \tag{47}$$

Remains in $S_t$ for all $t\in(t_0,\ t_1)$, that is

$$z(t)\ =\ h\ (x(t)\ ,\ t)\ ,\ t\in(t_0,\ t_1) \tag{48}$$

This definition furnishes a condition which can be used to verify whether $h(x,t)$ in (44) defines an integral manifold of(45)-(46).

***Manifold condition:*** If $h\ (x,t)$ satisfies the partial differntial equation:

$$\frac{\partial h}{\partial t}+\frac{\partial h}{\partial x}f(x,h(x,t),t)=g(x,h(x,t)t) \tag{49}$$

the surface $S_t$ given by (44) is an integral manifold of the dynamic system (45)-(46). This condition is simply obtained by differentiting (48) with respect to $t$:

$$\dot{z} = \frac{\partial h}{\partial t} + \frac{\partial h}{\partial x}\dot{x} \tag{50}$$

and then substituting $x^{\bullet}$ and $z^{\bullet}$ from (45) to (46). Once the existence of an integral manifold $S_t$ of $D_t$ has been established and its defining function $h(x,t)$ has been found, then the restriction of $D_t$ to the manifold $S_t$ is given by the $s$ th-order system

$$\dot{x} = f(x, h(x,t), t), \qquad x \in R^s \tag{51}$$

which is obtained by the substation of $z=h(x,t)$ into (46).

In addition to being a tool for reduced order modeling, the concept of an integral manifold is also a decomposition tool. A reduced order model (51) is a correct description of the dynamic $D_t$ only when the intial state is in $S_t$, as in (47). When the initial state of $D_t$ is not in $S_t$, the knowledge of the manifold function $h(x,t)$ continues to be useful by allowing us to replace the $z$-coordinates by the "off-manifold" coordinates $\eta$.

$$\eta = z - h(x,t) \qquad \eta \in R^m \tag{52}$$

In terms of the new coordinates $\eta$ and $x$ the original system (45) –(46) becomes:

$$\dot{\eta} = g(x, \eta + h(x,t), t) - \frac{\partial h}{\partial x} f(x, \eta + h(x,t), t) - \frac{\partial h}{\partial x} \tag{53}$$

$$\dot{x} = f(x, h(x,t), t) \tag{54}$$

An advantage of this full order description of $D_t$ over (45) –(46) is that now the manifold condition is simply $\eta=0$. The decomposition is achieved in the sense that on the surface $S_t$ the subsystem (53) is at an equilibrium: $\eta(t_0)=o$ implies $\eta(t)=0$ for all $t \in (t_0, t_1)$and all $x$. the "off-manifold " / " in-manifold" description (53)-(54) is particularly helpful when the in-manifold behavior of $D_t$ is of primary interest and the off-manifold variable is evaluated separately as a correction term. The analysis presented in the subsequent sections illustrates both conceptual and computational advantages of this nonlinear decomposition approach .

**4-2-Application to the Doig Model**

The integral manifolds theory outlined in the previous section was applied to the case of the DOIG detailed model .

Lets euation (40) for the fast transients be partitioned as

$$\begin{bmatrix} \dot{\eta}_{sw} \\ \dot{\eta}_{sc} \end{bmatrix} = \begin{bmatrix} K \ldots\ldots\ldots L \\ P \ldots\ldots\ldots Q \end{bmatrix} \begin{bmatrix} \eta_{sw} \\ \eta_{sc} \end{bmatrix} + \begin{bmatrix} R \\ T \end{bmatrix} v_1 \tag{55}$$

Here the predominant fast transients in $\eta_{sw}$ caused by the natural mode associated with the stator winding flux-linkage $\varphi_1$, are lightly damped and highly oscillatory. The preominant fast tranients in $\eta_{sc}$, caused by the natural mode associated with the second circuits rotor cage flux-linkage, $\varphi_3$ ,are heavily damped. In this section ,the state variable $\eta_{sc}$ related to second

circuts rotor is eliminated using integral manifolds.

According to integral manifolds theory that is defined in section 4-1 variables $x$ and $z$

$$x=[\eta_{sw}...\sigma_m.....s] \tag{56}$$

$$z=[\eta_{sc}] \tag{57}$$

and

$$\varepsilon=\tau_3=l/r_3$$

When $\tau_3$ is non zero but small, We let $\tau_3=\varepsilon$ and search for the unknown functions:

$$\eta_{sc}=h(\eta_{sc},\sigma_m,s\varepsilon) \tag{58}$$

Using two power series in $\varepsilon$ about $\varepsilon=0$, namely,

$$h=h_0+\varepsilon h_1+\varepsilon^2 h_2+.... \tag{59}$$

To find the terms $h_0,h_1,...$ of the series, we use the fact the function $h$ must satisfies(50). In view of (58), these give,

$$\varepsilon\frac{\partial h}{\partial \eta_{sw}}.\frac{d\eta_{sw}}{dt}+\varepsilon\frac{\partial h}{\partial \sigma_m}.\frac{d\sigma_m}{dt}+\varepsilon\frac{\partial h}{\partial s}\frac{ds}{dt}=(l/r_3)(P\eta_{sw}+Qh+Tv_1) \tag{60}$$

Which are partial defferential equations that must be satisfied by the series(59) as identities for all $\varepsilon$ near zero. With using (6), (37)and (55) and subsituating into (60), we obtain expersions in terms of $\varepsilon^0,\varepsilon^1,\varepsilon^2,...$ .

Equating coefficients of $\varepsilon$ gives the identities to be satisfied by each $h_i$ .Due to decompose $\eta_n$ and $\sigma_m$ ,the second term of left side (60) is zero. Also $s$ is very slowly in compare with other variables, so the third term of left side (60) is zero. For $h_0$ we equate all the terms not containing $\varepsilon$ giving,

$$h_0=-Q^{-1}P\eta_{sw}-Q^{-1}Tv_1 \tag{61}$$

Equating coefficients of $\varepsilon^1$ gives

$$h_1=-(r_3/l)Q^{-1}P[(K-LQ^{-1}P)\eta_{sw}+(R-LQ^{-1}T)v_1]$$

This process can be continued to obtain higher order terms if desired. Stopping with two terms, the approximate manifold experssion is,

$$h=\eta_{sc}=h_0+\varepsilon h_1 \tag{62}$$

therefore dynamic equations for the state variable related to second circuts rotor, $\dot{\eta}_{sc}$ are converted to algebric equations and detailed model is reduced order to fifth order. Equations (55) is rewrited as following:

$$\eta_{sw}^{\bullet} = K^{"}\eta_{sw} + R^{"}v_1 \tag{63}$$

where

$$K^{"} = K + LQ^{-1}P(I - K - LQ^{-1}P) \tag{64}$$

and

$$R^{"} = -LQ^{-1}T + LQ^{-1}P(R - LQ^{-1}T) + R \tag{65}$$

Thus, equations (6), (37)and (63)constitute a partially decomposed, reduced order model (fifth order) for the DOIG.

## 5- Linearized New Model

Each of the two nonlinear models full order and fifth order can be linearized around an operating point if it is assume that the variables have sufficiently small deviations from the operating point. For example this assumption is made in dynamic stability studies of power systems where it is customary to use a linearzied model so that linear system analysis methods can be conveniently applied.

The linearization process could be directly applied to the fifth order DOIG model. However, the coefficients of the resulting equations, particularly for the fifth-order model, would have rather complicated algebraic expressions. An equivalent approach is through linearizing the complete seventh order model and then numerically deriving the linearized fifth model by following process. Let the linearized and decomposed seventh-order equations be partitioned as

$$\Delta\eta_n^{\bullet} = A_{nmo}\Delta\eta_n + G_{nmo}\Delta v_1 \tag{66}$$

$$\Delta\sigma_m^{\bullet} = D_{nmo}\Delta\sigma_m - H_{nmo}\Delta v_1 + \Delta v_2 \tag{67}$$

$$\Delta s^{\bullet} = f(\Delta\varphi_{1d}, \Delta\varphi_{1q}, \Delta\varphi_{2d}, \Delta\varphi_{2q}, \Delta\varphi_{3d}, \Delta\varphi_{3q}, \Delta s) \tag{68}$$

Where $\Delta$ is small deviation in operating point. Linearized equations (55) rewriten as

$$\Delta\eta_{sw}^{\bullet} = K_O\Delta\eta_{sw} + L_O\Delta\eta_{sc} + R_O\Delta v_1 \tag{69}$$

$$\Delta\eta_{sc}^{\bullet} = P_O\Delta\eta_{sw} + Q_O\Delta\eta_{sc} + T_O\Delta v_1 \tag{70}$$

Thus, for the fifth-order model, $\Delta\eta_{sc}$ represents the second rotor circuit flux linkage. For a linear time invariant system, the integral manifold is sought in the from[12]

$$\Delta\eta_{sc} = E\Delta\eta_{sw} + q(\Delta v_1) \tag{71}$$

The substitution (71) in to (69) and (70) yeilds:

$$\begin{aligned} &E[K_O\Delta\eta_{sw} + L_O[E\Delta\eta_{sw} + q(\Delta v_1)] + R_O\Delta v_1] = \\ &Q_O[E\Delta\eta_{sw} + q(\Delta v_1)] + P_O\Delta\eta_{sw} + T_O\Delta v_1 \end{aligned} \tag{72}$$

Collecting the $\Delta\eta_{sw}$-dependent terms we require that the constant matrix $E$ be a solution

of

$$EK_O - Q_O E + EL_0 E - P_O = 0 \tag{73}$$

With such a $E$, the $\Delta v_1$-dependent terms require that

$$[Q_O - EL_O]q(\Delta v_1) + [T_O - ER_O]\Delta v_1 = 0 \tag{74}$$

which provided $(Q_O - EL_O)^{-1}$ exists, is satisfies by

$$q(\Delta v_1) = (Q_O - EL_O)^{-1}[T_O - ER_O]\Delta v_1 \tag{75}$$

The description of the system (69) and (70) restricted to the manifold (71) is given by the reduced order model:

$$\Delta\eta_{sw}^{\bullet} = [K_O + EL_O]\Delta\eta_{sw} + [L_O(Q_O - EL_O)^{-1}(T_O - ER_O) + R_O]\Delta v_1 \tag{76}$$

If initial conditions for $\Delta\eta_{sw}$ and $\Delta\eta_{sc}$ satisfies in (71), thus, reduced order model is (76), But if intial conditions don't meet manifold conditins, we seek expression similar to nonlinear model.

The accuracy of the linearized reduced-order moder can be verified by comparing the sets of bode diagram with that of the linearized full-order model at the operating point since the set of bode diagram of a linear time-invariant system generally characterizes the system transient behavior.

## 6-Simulation Algorithm

The decomposed, reduced order model consists of three sets of differential equations, i.e., (63) for the fast state $\eta_{sw}$, (37) for the slow sate $\sigma_m$, and (6) for he very slow slip $s$. These can be solved with different integration time steps, say $\Delta t$, $M*\Delta t$ and $N*\Delta t$ respectively. The integers $M$ and $N(N>M>1$, and $(N/M)$ is a integer ) are selected in accordance with the response speeds of the associated states.

At first the fast and slow variables are initialized as $\eta_{sw}^{o}$ and $\sigma_m^{o}$, the matrices $D_{nm}$, $H_{nm}$, $R^{"}$ and $K^{"}$ are formed using initial slip value. Then, $\eta_{sw}(t+\Delta t)$ is computed $M$ times using time step $\Delta$t. Next, $\sigma_m(t+\Delta t)$ is calculated using time step M*$\Delta$t. This set of variables is calculated $(M/N)$ times. Then the slip, $s(t+N*\Delta t)$, is determined using time step $N*\Delta t$, along with updating the matrices $D_{nm}$, $H_{nm}$, $R^{"}$ and $K^{"}$ with the new slip.

## 7-Model Validation

### 7-1-Simulation

To validate the procedure, the decomposed, reduced order new model response was compared to that of the original full order, reduced order model using singular perturbation theory and reduced order with quasi steady state .i.e. $\varphi_3^{\bullet} = 0$. The model parameters listed in appendix. The iterative separation procedure was carried out for only one full iteration, i.e. $n=m=1$, The basic time step $\Delta$t for the fast variable and for the full order model was taken equal to 0.0004 s. furthermore, M and N were seleced to be 5 and 50 respectively so that the slow variable time step is 0.002 s and the time step for the slip is 0.02 s. Fourth order Runge kutta integration method was used.

The relevant variables are generally the instantanous active and reactive power flows, at the machine terminals, speed and electromagnetic torque obtained respectively from

$$p = v_{1d}i_{1d} + v_{1q}i_{1q} + v_{2d}i_{2d} + v_{2q}i_{2q} \tag{77}$$

$$Q = v_{1q}i_{1d} - v_{1d}i_{1q} + v_{2q}i_{2d} - v_{2d}i_{2q} \tag{78}$$

$$\omega_r = (1-s)\omega \tag{79}$$

A start-up corresponding to mechanical torque increase 0 to %100 is simulated for the different nonlinear models and the behaviors of active power, reactive power, speed and electromagnetic torque are shown in fig. 2.

The second selected case study targets the simulation of a fault in the a.c. system which causes the voltage dip in generator terminal at 50 msec and normal operation occurring 500 msec after which normal operation voltages was restored. Fig. 3. shows the active and reactive power flows, speed and electromagnetic torque for the different normal models.

These simulations are confirmed, the defined method in this paper is more carefull than other methods.

The another note is speed simulation. Due to fast and slow modes is decoupled, the nessessry simulation time less than other methods .In table 1 simulation speed for all of methods is compared.

**7-2-Experiment**

The dynamic behavior of a 11 kw two pole DOIG machine was invesigated in the laboratory. The parameters of the machine are given in appendix. The DOIG machine was attached to a dc machine via a torque transducer. The dc machine was fed by a four quadrant thyristor converter and could, thus produce any desired shaft torque variations. The DOIG machine was connected to an autonomous grid, created by means of a forced commutated IGBT converter. The converter kept the voltages constant regardless of the currents of the DOIG machine, i.e., it componsated and the blanking time. Another feature of the IGBT converter was that it could generate desired deviations in the frequency and magnitude of the supply voltage.

The rotor speed was measured by an analog tachometer attached to the dc machine, while the currents and voltages were measured transducer with a high bandwith. The active and reactive powers, as well as the stator voltages and currents in field coordinates, were determined on line. The shaft torque was measured by meane of the torque transducer, and the dc machine torque was determined by measuring the armature current of the machine.

Small sinusodial perturbations in the frequency or magnitude of the voltage were generated by controlling the IGBT converter, and torque perturbations were generated by controlling the four quadrant thyristor converter. The gains and phase shifts of the different transfer functions we determined based on measured signals.

The electrodynamic torque could not be measured directly. Since the moments of inertia of the two rotating machines and electrodynamic torque of the dc machine were known, it was possible to determine the variations in the electrodynamic torque of the DOIG machine from the measured shaft torque.

**7-3-Comparsion of Simulation and Measurments**

The rotor speed, electrodynamic torque, active power, reactive power and the stator current response to shaft torque, voltage and frequency perturbations were measured and compared with theoretical results. A selection of measured and calculated responces is presented in Fig

4-7.

Fig. 4 shows the rotor speed response ($\Delta\omega_r$) to supply frequency perturbations($\Delta\omega_s$), Fig. 5 and 6 show the active power response($\Delta P$) and the reactive power response ($\Delta Q$) to voltage magnitude perturbations ($\Delta v$), and Fig. 7 shows the electrodynamic torque response ($\Delta T_e$) to shaft torque perturbations($\Delta T_l$).

In these measurment, the flux linkage in the machine was reduced from the nominal one in order to reduce the effects of magnetic saturation in the model comparsion. Terefore, the ac voltage selected was 250 V and supply frequency was 44 Hz. The static shaft torque was 51 Nm in DOIG operation.

The new fifth order model was validated agaisnt the measured results.

**Table (1)**

| model | Simulation speed(%) |
|---|---|
| Full order | 100 |
| Quasi steady state | 125 |
| Singular perturbation | 140 |
| New model | 146 |

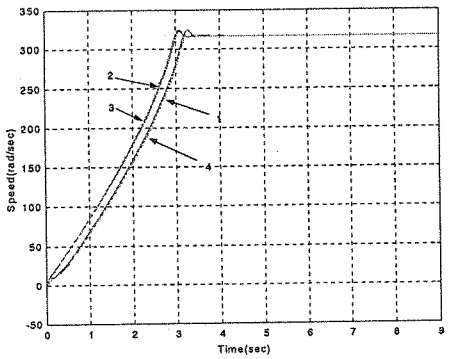


**Figure (2 a) DOIG rotor speed response at start-up (1) detailed model, (2) quasi steady state model, (3) sigular perturbation model, (4) new model**

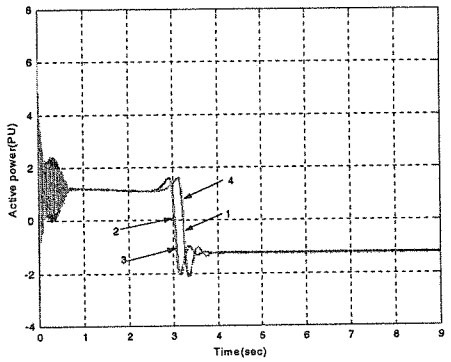


**Figure (2b) DOIG active power response at start-up (1) detailed model, (2) quasi steady state model, (3) sigular perturbation model, (4) new model**

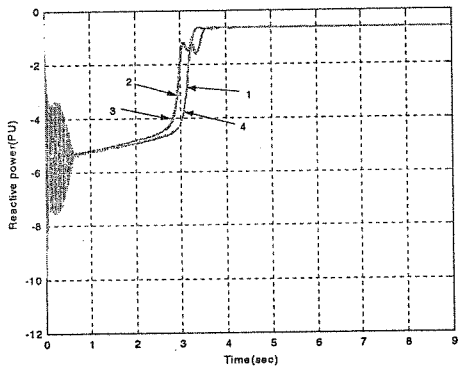


**Figure (2c) DOIG reactive power response at start-up (1) detailed model, (2) quasi steady state model, (3) sigular perturbation model, (4) new model**

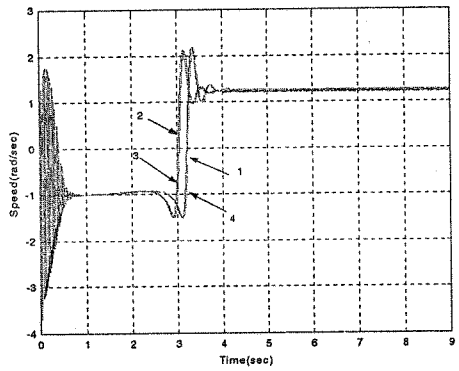


**Figure (2d) DOIG Electromagnetic Torque response at start-up (1) detailed model, (2) quasi steady state model, ( 3)sigular perturbation model, (4) new model**

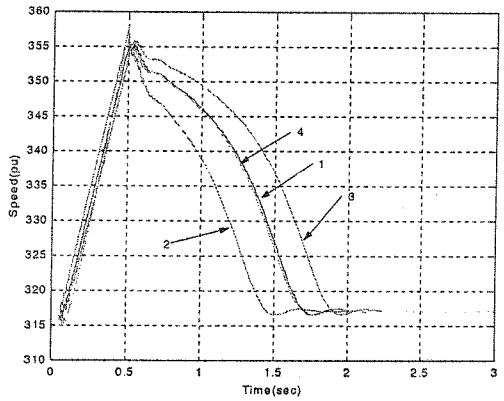


Figure (3 a) DOIG rotor speed response to temporary three phase fault (1) detailed model, (2) quasi steady state model, (3)sigular perturbation model, (4) new model

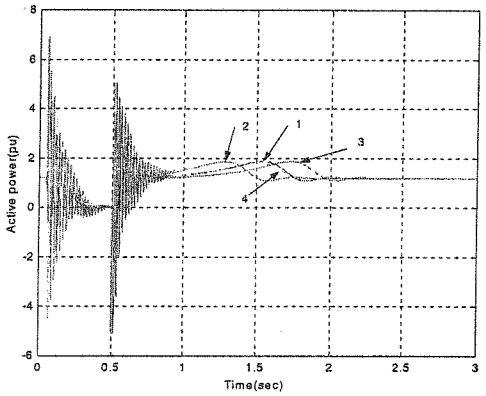


Figure (3b) DOIG active power response to temporary three phase fault (1) detailed model, (2) quasi steady state model, ( 3)sigular perturbation model, (4) new model

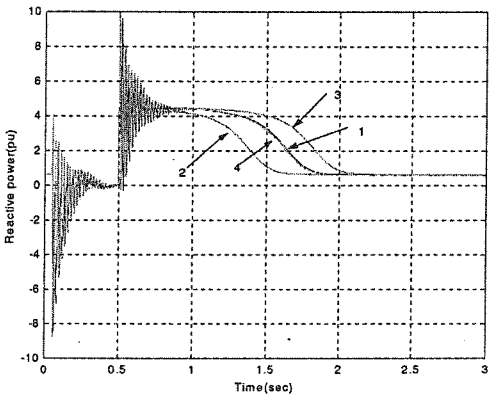


Figure (3c) DOIG reactive power response to temporary three phase fault (1) detailed model, (2) quasi steady state model, (3) sigular perturbation model, (4) new model.

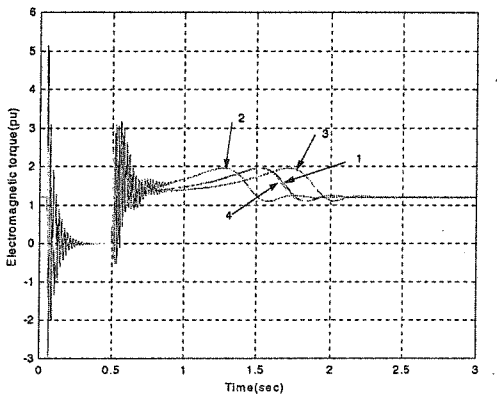


Figure (3d) DOIG Electromagnetic Torque response to temporary three phase fault (1) detailed model, (2) quasi steady state model, (3) sigular perturbation model, (4) new model.

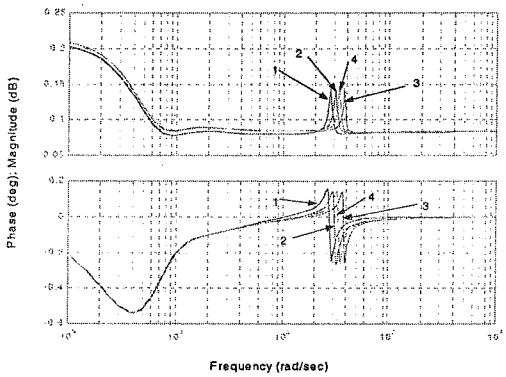


Figure (4) Measured and calculated gains and pase shifts of $(\Delta\omega_r / \Delta\omega_s)$.

(1) detailed model, (2) measured model, (3) sigular perturbation model, (4) new model.

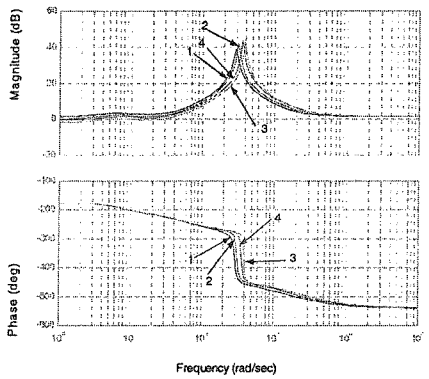


Figure (5) Measured and calculated gains and pase shifts of $(\Delta P / \Delta v)$ (1) detailed model,

2) measured model, ( 3) sigular perturbation model, (4) new model.

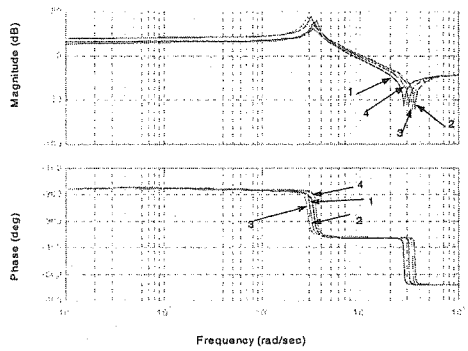


**Figure (6) Measured and calculated gains and pase shifts of $(\Delta Q/\Delta v)$ .(1) detailed model, (2) measured model, (3) sigular perturbation model, (4) new model**

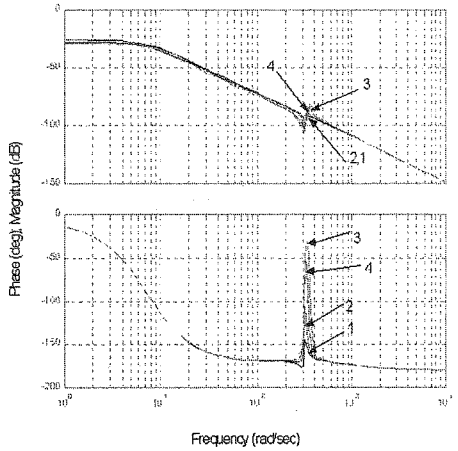


**Figure (7) Measured and calculated gains and pase shifts of $(\Delta T_e/\Delta T_l)$ . (1) detailed model,(2) measured model, (3) sigular perturbation model, (4) new model**

## 8-Conclusion

The simulation results show that the decomposed, reduced order model of a DOIG using integral manifold adequately reproduces the original model responses to typical power system voltage conditions. Implementing the separation procedure through one complete iteration proved to be sufficient to produce results almost identical to those of the original model.

The program used for comparing the computer simulation showed a speed advantage of better than other models for the modified model over the original model.

Furthermore, since the equations for the fast and slow variables are completely decoupled, parallel processing may be used to advantage.

Because of improved computational efficiency, the modified model may be used in studies where machine stator and network transients must be included but where long term behavior is also of interest.

## Appendix

### A- Nomenclature

$l_m, l$ - magnetizing inductance and dynamic inductance

$r$,- resistance

$v, i, \varphi$ - instantaneous values of voltages, currents and flux linkages

$\omega_r$ - angular velocitie of rotor(electrical)

$H$ - inertia coefficient

$T_m, T_e$ - mechanical torque and machine torque

$s$ - slip

$\omega$ - stator angular frequency

*1,2,3*- subscripts for stator winding ,rotor first and second winding

## *B-Model Parameters (STATOR CIRCUIT)*

*TABLE.II.Charactristics of DOIG used in calculations*

| DOIG Charactristic | Value |
|---|---|
| Base voltage | 400V |
| Base MVA | 11 KW |
| Base Frequency | 50 Hz |
| Stator resistance( $r_1$ ) | 0.032 pu |
| Stator leakage inductance( $l_1$ ) | 0.093 pu |
| First winding resistance( $r_2$ ) | 0.022 pu |
| First winding leakage inductance( $l_2$ ) | 0.1 pu |
| Second winding resistance( $r_3$ ) | 2.2 pu |
| Second winding leakage inductance( $l_3$ ) | 1.1 pu |
| Magnetizing inductance( $L_m$ ) | 2.1 pu |
| Lumped inertia coefficient(J) | 0.073 sec |
| Recovery transformer turns ratio | 0.733 |

**C-Auxliary Equations**

The inductance matrix $l$ in

$$\varphi = li \tag{c-1}$$

is writen as

$$l = -\begin{bmatrix} l_1 + l_m \ldots\ldots\ldots l_m \ldots\ldots\ldots l_m \\ l_m \ldots\ldots\ldots\ldots l_2 + l_m \ldots\ldots l_m \\ l_m \ldots\ldots\ldots\ldots l_m \ldots\ldots\ldots l_3 + l_m \end{bmatrix}. \tag{c-2}$$

So that

$$i = L^{-1}\varphi \tag{c-3}$$

with

$$L^{-1} = (-1/l)\begin{bmatrix} l_{11} \ldots\ldots\ldots - l_3 l_m \ldots\ldots\ldots - l_2 l_m \\ - l_3 l_m \ldots\ldots\ldots l_{22} \ldots\ldots\ldots - l_1 l_m \\ - l_2 l_m \ldots\ldots\ldots - l_1 l_m \ldots\ldots\ldots l_{33} \end{bmatrix} \tag{c-4}$$

where

$$\begin{aligned} l_{11} &= l_2 l_3 + l_2 l_m + l_3 l_m \\ l_{22} &= l_1 l_3 + l_1 l_m + l_3 l_m \\ l_{33} &= l_1 l_2 + l_1 l_m + l_2 l_m \\ l &= l_1 l_2 l_3 + l_1 l_2 l_m + l_1 l_m l_3 + l_m l_2 l_3 \end{aligned} \tag{c-5}$$

## References


[1] Bansal, R.C.; Bhatti, T.S.; Kothari, D.P. "Bibliography on the application of induction generators in nonconventional energy systems", *IEEE Transactions on Energy Conversion, Volume: 18 No: 3, Sept. 2003, Page(s): 433 –439*

[2] H.D. Battista, P.F.Puleston, R. J. Mantz,C. F. Christiansen, "Sliding mode control of wind energy systems with DOIG-power efficiency and torsional dynamics optimization", *IEEE Trans. Power Systems,*, vol. 15, pp. 728734, May 2000.

[3] J. B. Ekanayake, L. Holdsworth, X. Wu, N. Jenkins,"Dynamic Modelling of Doubly Fed Induction Generator Wind Turbines", *IEEE Trans. On power systems, VOL.18, No .2, May 2003, pp.803-809*

[4] N. Gunarathnam, D. W. Novotny, "The effect of neglecting stator transients of induction machines in dynamic stability studies", IEEE T-PAS-99 PP.2050-2059,Nov 1980

[5] E. Levil, D. Rauski, "Self excitation modeling in deep bar and double cage induction generators", IEEE.....

[6] Rui M.G. Castro, J.M.Ferreira de jesus, A wind park linearized model ", *proc.1993 British wind Energy association conf. (BWEA), York Oct. 1993.*

[7] J.M. Undrill, A.E. Turner, "Construction of power system electromechanical equivalents by modal analysis". *IEEE Trans. On power apparatus and systems . Vol. PAS-90 , Sep/Oct.1971.*

[8] Bruce C.Moore, "Principal Component Analysis in linear systems: Controllability, Observability, and model reduction ", *IEEE Trans. On automatic control, Vol.AC-26 , No. 1, Feb.1981.*

[9] Peter M.M.Bongers ,"Modeling and Identification of flexible wind turbines and factorizational Approach to robust control ", *PhD Thesis, Delft University of technology, Delft University of technology, Delft. Jun.1994.*

[10] Castro, R.M.G.; Ferreira de Jesus, J.M.; "A wind park reduced-order model using singular perturbations theory," *IEEE Transactions on Energy Conversion, Volume:11, No:4, Dec.1996, Page(s): 735 –741*

[11] G. Richrds, O.T. Tan, "Decomposed, reduced order model for double cage induction machines", *IEEE T-EC-1, No.3, Sept. 1986, pp. 87-93*

[12] Tseng, H.C.; Kokotovic, P.V.; "Tracking and disturbance rejection in nonlinear systems: the integral manifold approach", *Proceedings of the 27th IEEE Conference on Decision and Control, 1988., 7-9 Dec. 1988,Page(s):459-463,vol.1*

[13] Sedighizadeh. M., Kalantar, M; "A wind farm reduced order model using Integral manifold theory," *IASTED conf. MIC 2004, 23-25 Feb 2004,grindelwald, switzerland , pp.281-286*